

## A quantitative description of thermal transport in the SOL of ASDEX Upgrade

D. Carralero<sup>1</sup>, S. Artene<sup>1</sup>, G. Birkenmeier<sup>1,2</sup>, M. Faitsch<sup>1</sup>, P. Manz<sup>1,2</sup>, P. deMarne<sup>1</sup>, B. Sieglin<sup>1</sup>, U. Stroth<sup>1</sup>, N. Vianello<sup>3,4</sup>, M. Wischmeier<sup>1</sup>, E. Wolfrum<sup>1</sup>, the ASDEX Upgrade team and the EUROfusion MST1 Team<sup>5</sup>.

<sup>1</sup> Max-Planck-Institut für Plasmaphysik, Garching, Germany. <sup>2</sup> Physik-Department E28, Technische Universität München, Garching, Germany. <sup>3</sup> Consorzio RFX (CNR, ENEA, INFN, Università di Padova, Acciaierie Venete SpA), Corso Stati Uniti 4, 35127 Padova, Italy <sup>4</sup> Swiss Plasma Center (SPC), EPFL Lausanne, Switzerland, <sup>5</sup> See the author list of H. Meyer et al, Overview of progress in European Medium Sized Tokamaks towards an integrated plasma-edge/wall solution, accepted in Nuclear Fusion

The need to predict of heat fluxes into the different plasma facing components represents a serious requirement for the design of a reactor-relevant tokamak. While substantial experimental effort has been dedicated to the evaluation of convective particle fluxes associated to filaments [1], few works have attempted to provide a quantitative description of the perpendicular and parallel heat fluxes in the far SOL, and their relation to filamentary transport. A widely accepted picture of SOL thermal transport assumes that most of the power crossing the separatrix,  $P_{\text{SOL}}$ , is immediately transferred to the targets by electron conduction, thus leading to extremely low  $\lambda_q$  values in the divertor typically in the range of a few mm. However, this simplified picture fails to account for two important facts: first, it assumes  $T_i \approx T_e$ , across the whole SOL. This has been proven false by experiments in many tokamaks [2,3,4], where values in the  $\tau_i = T_i/T_e \sim 2\text{-}5$  range have been measured. Second, it does not take into account the effect of enhanced perpendicular transport associated to filaments either. In this work, we set out to analyse these subjects: By combining data from different L-mode experiments [4,5] carried out in equivalent plasma configurations in AUG, we have created a data base of all relevant SOL plasma parameters including  $n_e$ ,  $T_e$  and  $T_i$ , filament velocity, parallel Mach number, etc., which allows for a quantitative estimation of heat fluxes in the SOL.

From the available data, two sets have been separated using the divertor collisionality parameter  $\Lambda_{\text{div}}$ , which has been experimentally related to density shoulder formation [5]. Low collisionality discharges ( $\Lambda_{\text{div}} < 0.5$ ) feature no shoulder in the midplane, and are in the low recycling, conduction limited regime in the divertor. Instead, high collisionality ones ( $\Lambda_{\text{div}} > 3$ ) have already developed a density shoulder and transitioned into the high recycling

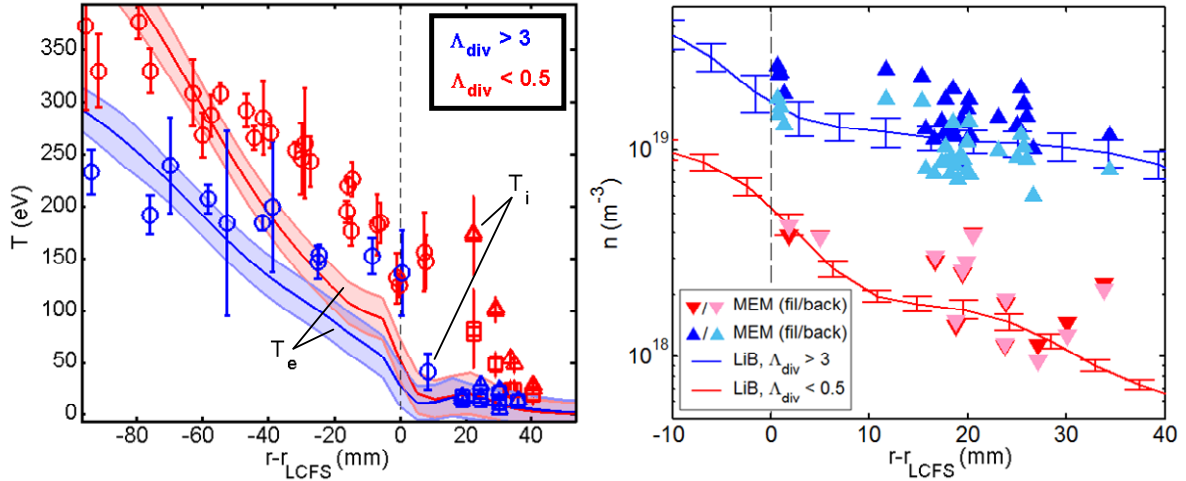


Figure 1: Left, temperature measurements in AUG edge. Symbols/lines represent  $T_i/T_e$ .  $\circ$  are CXRS data, and  $\Delta/\square$  represent filament/background RFA measurements. Right, comparison between filament/background density measurements carried out in the SOL by the MPM and typical LiB profiles. In all cases red/blue stands for low/high collisionality.

regime, with a partially detached divertor. Both kinds of discharges feature  $\tau_i > 1$  and  $\tau_i \sim 3$  for the last 50 mm before and at the separatrix. This is shown in Figure 1, where Thomson Scattering, ECE and swept Langmuir probe (LP) data are combined to produce  $T_e$  IDA profiles, and CXRS and RFA probes are combined to produce  $T_i$  profiles. However, while  $T_e$  drops to around 15 eV within the first 5 mm in the SOL in both cases,  $T_i$  decays over longer scales. In particular,  $\lambda_{T_i} \sim 30$  mm for low collisionality. This leads to an even higher  $\tau_i \sim 5$  for  $r-r_{LCFS} \sim 10$  mm. From these temperature profiles,  $T_e$  and  $T_i$  values are interpolated for experiments in which the midplane manipulator (MPM) was equipped with a multipin probe designed to measure filament size and velocity. In order to assess the reliability of such interpolations, density values are calculated from ion saturation current ( $I_{sat}$ ) measurements for filaments and background, carried out by LP in the MPM and compared with the corresponding LiB profiles. As can be seen in Figure 1, the agreement is very good, with LiB data falling between MPM filament and background levels both for high and low  $\Lambda_{div}$  values.

A more direct validation of the combination of temperature profiles and LP measurements for the calculation of heat fluxes can be done by using them to calculate the heat delivered to the MPM probehead and comparing it to a direct observation carried out with an infrared (IR) camera. Indeed, the power reaching the wall of the probe is

$$q_W = \frac{I_{sat}}{A_{probe} Z e} (T_e [\gamma_i \tau_i (1 - R_E) + \gamma_e] + E_{rec})$$

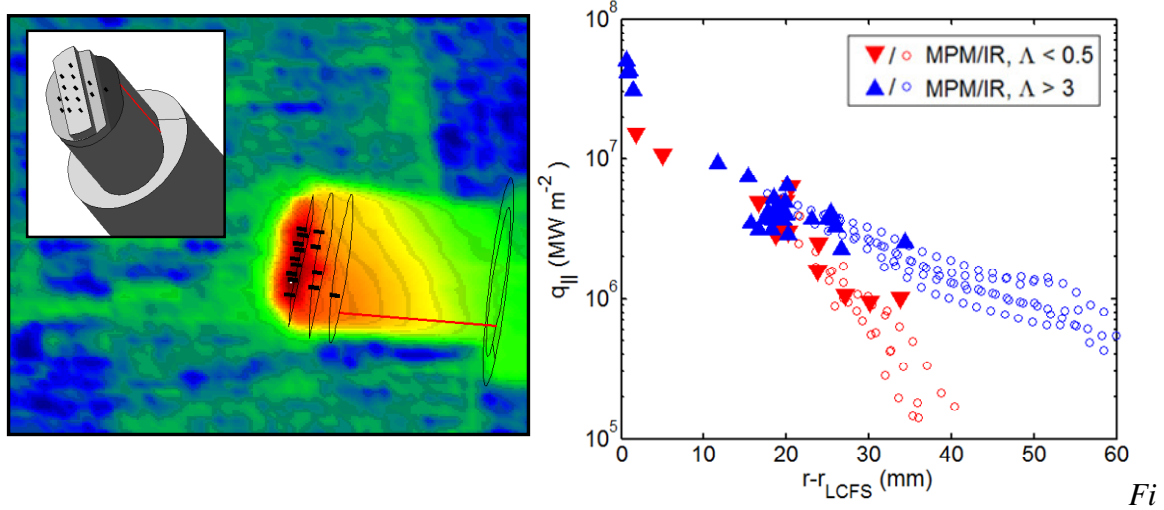


Figure 2: Left,  $q_{||}$  derived from the IR data (au.). The outline of the 3D model of the probehead shown in the insert is projected for reference, including the radial profile of points with perpendicular  $B$  incidence, in red. Right,  $q_{||}$  profiles calculated from IR and probe data.

where  $\gamma_i \sim 5$ ,  $\gamma_e \sim 2$ ,  $A_{\text{probe}}$  is the collection area of the probe,  $E_{\text{rec}}$  is the recombination energy and an energy reflection coefficient,  $R_E \sim 0.5$  was used for a tungsten surface [6]. The power to the probe head can also be calculated from IR data using the THEODOR code [5]. In Figure 2, the radial  $q_w$  profiles from IR data are compared to probe data for high and low collisionalities. As can be seen, the agreement between the two power flux estimates is remarkable. The power delivered to the wall is similar for both cases at  $r-r_{\text{LCFS}} \sim 20$ , but further away from the separatrix, the effect of the shoulder formation can be seen as an increase on the power decay length, suggesting an enhanced perpendicular to parallel heat transport ratio.

Finally, global transport in the SOL is evaluated using the database: for a given  $r-r_{\text{LCFS}}$ , the total perpendicular transport can be estimated [7] as that crossing the area,  $S_{\text{mid}}$ , defined by that magnetic surface in the midplane (defined by a poloidal angle of  $-45^\circ < \varphi < 45^\circ$ , corresponding to the MPM position at  $\varphi \sim 45^\circ$ ):

$$Q_{\perp} = \left[ \frac{5}{2} (\Gamma_{\perp, \text{fil}} (T_{i, \text{fil}} + T_{e, \text{fil}}) + D_{\text{Bohm}} \nabla_{\perp} n (T_{i, \text{back}} + T_{e, \text{back}})) + \frac{1}{2} \Gamma_{\perp} m_D (c_s M)^2 \right] S_{\text{mid}}$$

where  $\Gamma_{\perp, \text{fil}}$  is the perpendicular particle convection associated to filaments,  $M$  is the parallel Mach number and Bohm coefficients have been used to estimate diffusion. The results are displayed in Figure 3, where  $Q_{\perp}$  is normalized to  $P_{\text{SOL}}$ . As was to be expected,  $Q_{\perp} \sim P_{\text{SOL}}$  at the separatrix. Also, the same similarity and departure is observed between the low and high  $\Lambda_{\text{div}}$  cases at 20 mm and beyond as in Figure 2. Most importantly, it can be seen that 20-25% of the power crossing the separatrix still remains at the midplane for  $r-r_{\text{LCFS}} \sim 20$  mm. Finally, the SOL power balance at the

midplane can be estimated [7] by comparing  $Q_{\perp}$  at each radius with the amount of power lost in the parallel direction,  $Q_{\parallel}$ , between the separatrix and  $r$ , at the MPM position ( $\varphi = \pm 45^{\circ}$ , defined as the poloidal limit of the domain):

$$Q_{\parallel}(r) = 2\pi \int_{r_{LCFS}}^r \sum_{\alpha=e,i} \left[ \frac{2}{7} \kappa_{\alpha} \frac{T_{\alpha}^{7/2} - T_{div}^{7/2}}{L_{\parallel}} + \frac{1}{2} n c_s M (5T_{\alpha} + m_{\alpha} (c_s M)^2) \right] \frac{B_z}{B} dr$$

where  $\tau_i = 1$  has been assumed at the divertor [5], and  $L_{\parallel} = 1/5 L_c$  has been taken in the conduction limited case. Far from the separatrix,  $Q_{\parallel}$  should match the total power lost in the parallel direction  $P_{\parallel}$  (the total power collected at the divertor plus that radiated in the SOL) are shown along with  $P_{SOL}$ . These estimations yield sensible results, as  $Q_{\perp} \sim P_{SOL}$  at  $r=0$  and  $Q_{\parallel} \sim P_{\parallel}$  at  $r = 35$  mm within a 20% error. The main result is that, given the much larger parallel gradients (proportional to  $\tau_i^{7/2}$ ), ion transport dominates not only in

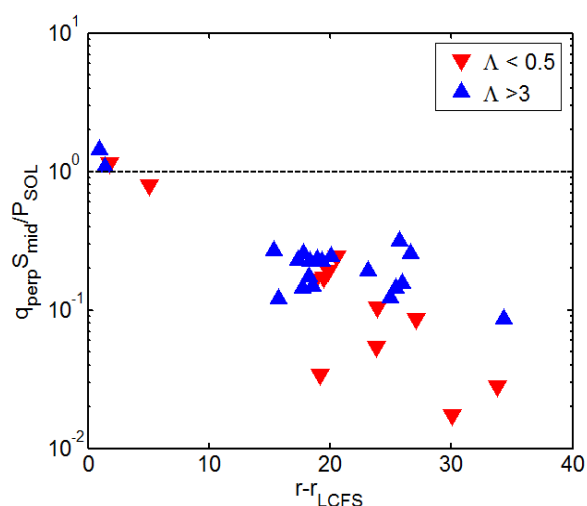


Figure 3: Total perpendicular power crossing  $S_{mid}$ , normalized with  $P_{SOL}$

the perpendicular, but also in the parallel direction. Again, large fractions of  $P_{SOL}$  are still present in the SOL for the first 15-20 mm after the separatrix. When the shoulder is formed, a non-negligible perpendicular component can be seen as far as 35 mm in front of the separatrix (composed by ion and electron convection components of roughly similar value). These results

should be taken into consideration when assessing plasma-wall interaction aspects such as divertor loads or main wall sputtering of next generation tokamaks, by discussing not only their  $P_{SOL}$  expected values, but also how such values will be divided between the electron and ion channels.

*This work has been carried out within the framework of the EUROfusion Consortium and has received funding from the Euratom research and training programme 2014-2018 under grant agreement No 633053. The views and opinions expressed herein do not necessarily reflect those of the European Commission.*

[1] D'Ippolito D.A., Myra J.R. and Zweben S.J. 2011 *Phys. Plasmas* 18 060501, [2] D. Carralero, M. Siccinio, M. Komm, et al., *Nucl. Fusion* 57 (2017) 056044 [3] M. Kocan, J.P. Gunn, S. Carpentier-Chouchana, et al. *Journal of Nuclear Materials* 415 (2011) S1133–S1138 [4] S. Elmore, S. Y. Allan, A. Kirk, et al. *Plasma Phys. Control. Fusion* 54 (2012) 065001 [5] D. Carralero, G. Birkenmeier, H.W. Müller, et al. *Nucl. Fusion* 54 (2014) 123005 [6] D. Brida, T. Lunt, M. Wischmeier, et al. Accepted for publication in *Nucl. Fusion* (2017) [7] Stangeby P. 2000 *The Plasma Boundary of Magnetic Fusion Devices* (Bristol: Institute of Physics Publishing)